 SL, vol.2, no.1, pp.49-62, 2009

A Novel Quadrant Array for Material Characterization and SHM of Orthotropic Plate-like Structures

J Vishnuvardhan[1], C V Krishnamurthy[2] and Krishnan Balasubramaniam[1]

Abstract: A novel small footprint sensor patch (single-quadrant double-ring Single-Transmitter Multiple-Receiver (STMR) array) has been developed and demonstrated successfully for the simultaneous reconstruction of the elastic moduli, material symmetry, orientation of principal planes and defect imaging. The sensor array contains a single transmitter in the center of the array and two sets of receivers at two different radii on a single quadrant. A slowness based reconstruction algorithm is used to determine elastic moduli from measured fundamental Lamb wave mode velocities using the direct received signals at different angles in a quadrant. A method proposed by Cowin and Mehrabadi (1987) is used to determine material symmetry and orientation of principal planes. Imaging is carried out with a phased addition algorithm and the reconstructed elastic moduli using the signals from flaws and structural features. To show the applicability of the method, simulations were carried out to image defects with the single-quadrant double-ring STMR array configuration and are compared with the images obtained using simulation data of the full-ring STMR array configuration. The experimental validation has been carried out on a 3.15 mm thick quasi-isotropic graphite-epoxy composite plate.

Keywords: Elastic Moduli, Health Monitoring, Phased Addition Algorithm, Genetic Algorithm.

1 Introduction

Composite structures are widely used in the aerospace industry due to various advantages such as (i) high strength-to-weight ratios, (ii) high stiffness-to-weight ratios, and (iii) their ability to be tailored material properties for specific applications. However, composite structures are susceptible to impact damage during service, which can cause internal damages (e.g. delaminations) or barely visible damages on the other side of the impact damaged surface. These damages are not visible

[1] Department of Mechanical Engineering, Indian Institute of Technology Madras, Chennai, India.
[2] Center for Nondestructive Evaluation, Indian Institute of Technology Madras, Chennai, India.

from the impact side, but manifest as serious delaminations on the other side. Additionally, disbond at the interface between the skin and the reinforcement (stiffener, ribs, etc.) is of particular concern, specifically in co-cured composite structures. Over a period of time, these damages can grow and lead to catastrophic failure of the structure. Hence, it is important to carry out non-destructive inspection of the composite structure frequently to identify the damages and assess the structural integrity.

The conventional non-destructive evaluation (NDE) techniques, such as ultrasonic C-scan, are not desirable to inspect the aerospace structural components due to (i) the localized inspection is inadequate and leads to time-consuming procedures for the whole structure, as the structures have large dimensions and complex geometry, (ii) they are expensive, and (iii) they are difficult to implement during service of the component. Hence, advanced methods such as structural health monitoring need to be studied.

1.1 Ultrasonic transducer array based Structural Health Monitoring (SHM)

SHM involves continuous monitoring of the changes in a structure with attached/-embedded network of sensors, and processing the acquired data to arrive at life cycle management decisions. It is an emerging field due to its vast potential for building-in reliability and safety into the structure as well as for reducing the inspection time and maintenance costs. A recent review of Structural Health Monitoring and Damage Detection with an emphasis on composite structures can be found in references Pawar and Ganguli (1997), Kuang and Cantwell (2003), Lynch and Loh (2006), and Montalvão, Maia, and Ribeiro (2006).

The greatest challenge in designing an SHM system is knowing what 'changes' to look for and how to identify them (Kessler, Spearing, and Soutis (2002)). Health monitoring of structures can be carried out by looking at (a) natural frequency of the structures [Kawiecki (1998)], (b) electromechanical impedance based measurement [Giurgiutiu, Zagrai, and Bao (2002); Giurgiutiu (2005)], (c) the strain based measurements [Zhou, Qiao, and Krishnaswamy (2006)], and (d) amplitude or energy of the ultrasonic signal reflected from edges and defects [Wilcox, Lowe, and Cawley (1999); Lin and Chang (2002); Wilcox (2003a); Wilcox (2003b); Ihn and Chang (2004); Qing, Kumar, Zhang, Gonzalez, Guo, and Chang (2005); Jagannathan, Balasubramaniam, and Krishnamurthy (2006); Soma Sekhar, Balasubramaniam, and Krishnamurthy (2006); Muralidharan, Balasubramaniam, and Krishnamurthy (2008)]. The present work uses ultrasonic signal amplitude information to monitor health of a structure.

It is expected that, a successful Structural Health Monitoring (SHM) approach should achieve large area coverage using a limited number of sensors fixed on to the

structure. Among the different health monitoring techniques, ultrasonic transducer array based techniques [Giurgiutiu, Zagrai, and Bao (2002); Giurgiutiu (2005); Wilcox, Lowe, and Cawley (1999)] are widely used for health monitoring of aircraft structures. Two prominent array based techniques are single-transmitter multiple-receiver (STMR) array, and multiple-transmitter multiple-receiver (MTMR) array for SHM of isotropic [Wilcox, Lowe, and Cawley (1999); Lin and Chang (2002); Wilcox (2003a); Wilcox (2003a)] and anisotropic structures [Jagannathan, Balasubramaniam, and Krishnamurthy (2006); Muralidharan, Balasubramaniam, and Krishnamurthy (2008)]. Array based techniques use algorithms that require prior knowledge of elastic moduli in order to compute the anisotropy in the material, and to calculate dispersion properties along different propagation directions. In all the above works, elastic moduli of virgin sample are used. Elastic moduli of a structure, at the time of carrying out SHM, may be different from the elastic moduli of virgin sample. Hence, there is a need to measure the elastic moduli in-situ and use the same for imaging defects as part of SHM.

In the present work, it is shown that a single sensor array is sufficient for in-situ measurement of elastic moduli as well as for in-situ health monitoring of anisotropic plate-like structures. The sensor array contains a single transmitter in the center of the array and two sets of receivers on a single quadrant at two different radii. Lamb waves are generated at the center of the array and are detected by the receivers at two different radii. Direct received signals are used in calculating the phase velocity, which in turn are used for the reconstruction of elastic moduli. The reflected signals are used to image the defects on the plate using phased addition algorithm.

The paper is organized as follows. Description of STMR array and the method of determining elastic moduli of anisotropic materials using Lamb wave phase velocities are explained in Section 2. Defect simulation procedure, phased addition algorithm, and two simulations to study the possibility of using single sensor array for elastic moduli determination and SHM of anisotropic plate-like structures are explained in Section 3. To validate the method, experiments have been carried out on 3.15 mm graphite-epoxy composite and are described in Section 4. Conclusions are presented in Section 5.

2 Array description and elastic moduli determination

A flexible Printed Circuit Board (PCB) based patch, "single-quadrant double-ring STMR array" was developed by bonding thin strain excitation based piezoelectric wafer-active sensors (PWAS) on a thin polyester film of Printed Circuit Board (PCB) and is shown in Fig. 1. Single-quadrant double-ring STMR array comprises of a transmitter in the centre of a circular ring and 20 receivers at 10 degree apart

on two radii (80 mm and 120 mm). PWAS [Giurgiutiu, Zagrai, and Bao (2002); Giurgiutiu (2005)] sensors of American Piezo Ceramic, APC 850, 1.0 mm thick and 10 mm diameter were used to generate and receive Lamb waves on anisotropic materials. PWAS have been used in SHM have several advantages such as (i) efficient Lamb wave generation and (ii) reduction in sensor weight and associated electronics. As shown in Fig. 2, the compact single-quadrant double-ring STMR array was attached to a 3.15 mm quasi-isotropic graphite-epoxy composite plate with honey as adhesive such that the same array can be used to characterize any other plates/plate-like structures. The 3.15 mm quasi-isotropic composite has been made from 21 unidirectional graphite-epoxy layers in the sequence of (+45, -45, 0, 90, 0, -45, +45)$_{3S}$.

For a material, whose elastic moduli are known, ultrasonic Lamb wave velocities of S_0 and A_0 modes can be calculated using Rayleigh-Lamb equations [Nayfeh (1995)]. If the experimentally measured S_0 and A_0 mode velocities are available, then the elastic moduli can be reconstructed by inverting the measured velocities by minimizing the error between experimental and calculated velocities. The inversion can be carried out in several ways. Recently we have shown that a Genetic Algorithm (GA) [Goldberg (1989)] based inversion method works well for the reconstruction of elastic moduli using ultrasonic Lamb wave velocities [Vishnuvardhan, Krishnamurthy, and Balasubramaniam (2007a)].

Experiments were carried out using MATEC PR5000 pulser-reciever to excite two cycles tone burst signal of 200 kHz from the central transmitter and to receive the propagated signals at two different radii (80 mm and 120 mm). NI SCXI-1000 multiplexer was used for multiplexing the receivers. The received signals were sampled at 20 Mega-samples/sec by using NI 5102 and then filtered using a band pass filter so that high frequency noise and undesirable low frequency components were eliminated. The received signals at two different radii were used in calculating the Lamb wave velocity. The procedure was repeated to determine Lamb wave velocities at each 10 degree propagation directions in that quadrant. The S_0 mode was used for elastic moduli reconstruction since this was the fastest mode and hence could be time gated. However the direct received A_0 mode signal could not be efficiently time gated because it was superimposed with the edge reflected S_0 mode signals. The difference in phase velocity and group velocity at this particular frequency-thickness *(fd)* product was very small and hence, the velocities obtained using experiments were considered as phase velocities and the reconstruction has been carried out. The elastic moduli reconstructed by inverting the experimental S_0 mode velocities are given in Tab. 1. The theoretical elastic moduli in Tab. 1 are calculated using the rule of mixtures with the elastic moduli of unidirectional graphite–epoxy composite given in paper [Vishnuvardhan, Krishnamurthy,

and Balasubramaniam (2007a)].

This elastic moduli reconstruction procedure is similar to the procedure defined elsewhere [Vishnuvardhan, Krishnamurthy, and Balasubramaniam (2009a)].Using the method proposed by Cowin and Mehrabadi [Cowin and Mehrabadi (1987)], it was found that, the material belongs to an orthotropic symmetry class with the principal axes matching with the geometric coordinate axes.

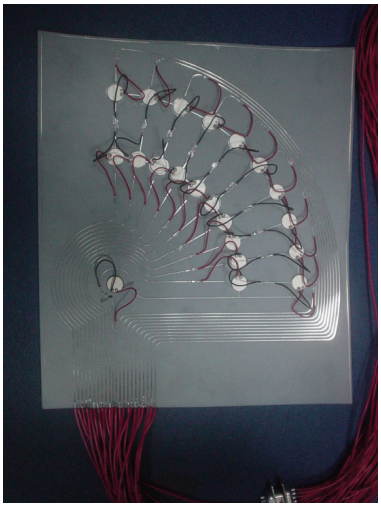

Figure 1: Snap shots of single-quadrant double-ring STMR array

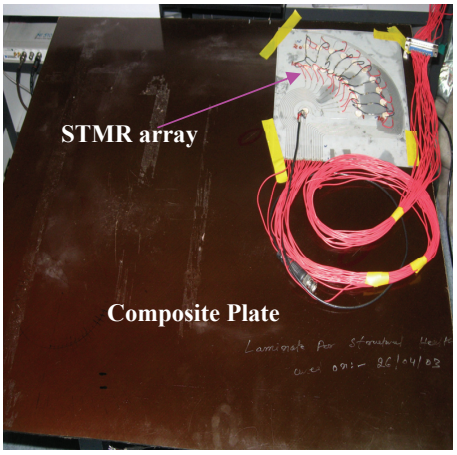

Figure 2: Single-quadrant double-ring STMR array on 3.15 mm quasi-isotropic graphite-epoxy composite

Table 1: Theoretical and Reconstructed elastic moduli (in GPa) of 3.15 mm graphite-epoxy composite using single-quadrant double-ring STMR array

Elastic Moduli	C_{11}	C_{12}	C_{13}	C_{22}	C_{23}	C_{33}	C_{44}	C_{55}	C_{66}
Theoretical	65.77	22.57	5.87	48.35	5.75	12.43	4.15	4.36	21.33
Reconstructed	61.51	22.02	5.95	47.15	5.80	12.76	4.08	4.13	19.42

3 PWAS Based Sensor array for in-situ SHM

Recent work on sensor array for the determination of elastic moduli of anisotropic plate-like samples has been encouraging [Vishnuvardhan, Krishnamurthy, and Balasubramaniam (2009a)]. PWAS was shown to be advantageous when dealing with

Lamb waves particularly in aerospace applications. Previously single-quadrant double-ring STMR array was used only for the in-situ assessment of elastic moduli where as the full-ring STMR array, shown in Fig. 3, was used for the health monitoring of anisotropic plate-like structures. Full-ring STMR array comprises of a transmitter in the centre of a circular ring and 36 equally spaced receivers at radius 60 mm. In this work, performance of the single-quadrant double-ring STMR array for the health monitoring has been carried out and compared with that obtained using full-ring STMR array. Details of the procedure for simulating the defects and to calculate the received signals at each receiver, and the phased addition algorithm for the reconstruction of defects were described elsewhere [Vishnuvardhan, Muralidharan, Krishnamurthy, and Balasubramaniam (2009b)].

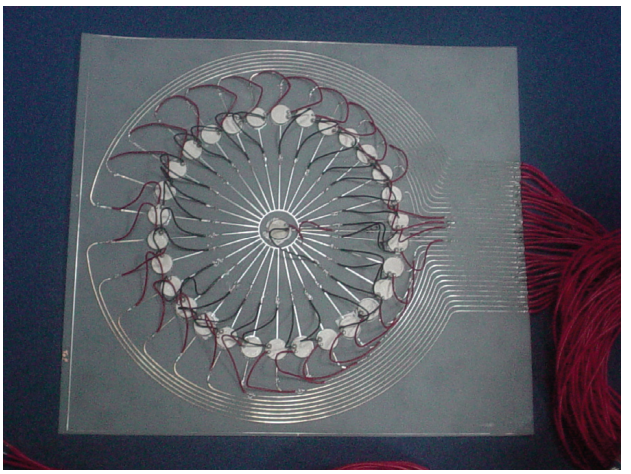

Figure 3: Snap shot of the full-ring STMR SHM array

3.1 Defect simulation procedure

Defects are simulated as point defects occupying one pixel in the object domain and are reconstructed using phased addition reconstruction algorithm. This algorithm takes into account the anisotropy in the material and performs phased addition reconstruction using dispersion data along various directions through which the Lamb wave modes propagate on the plate.

For simplicity, defect simulation procedure is explained for S_0 mode, and it can be readily applied for A_0 mode also. For a given plate, S_0 mode dispersion properties are calculated by solving Rayleigh-Lamb equation for the elastic moduli of

the plate. Using the dispersion characteristics, the signal at the j^{th} receiver is constructed from the path length (t_j) defined as the sum of the time of flights of wave propagating from transmitter to defect, and defect to j^{th} receiver at each of the frequencies present in the bandwidth of the excitation pulse, with the help of inverse FFT procedures.

3.2 Phased addition algorithm (PAA)

The phased addition algorithm reconstructs the position of reflectors, typically plate edges and defects, using the signals received by all the receivers. The flowchart [Jagannathan, Balasubramaniam, and Krishnamurthy (2006); Muralidharan, Balasubramaniam, and Krishnamurthy (2008)] of the phased addition algorithm is shown in Fig. 4. S_j(f) denote the spectra of the signal (T_j) received by j^{th} receiver. The algorithm starts by descretizing the image domain. For each image point (pixel) in the image domain, path lengths are calculated from transmitter to the pixel and from the pixel to each receiver. The received signals are back-shifted in time, in the frequency domain to counter the dispersion that has occurred as the wave travels from transmitter to the pixel and from the pixel to each receiver. The above procedure is repeated for each pixel in the image domain to calculate a matrix *A*. Then *A*is subjected to an Inverse Fast Fourier Transform to obtain a matrix *B* that contains the back shifted and phase added signals corresponding to each pixel in the image domain. The image matrix *O* can be constructed from matrix *B*.

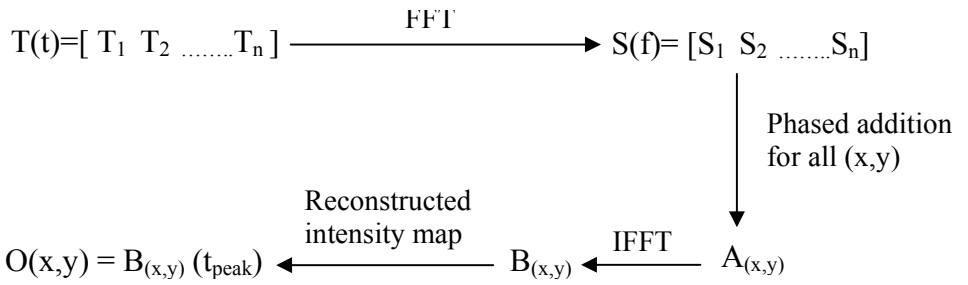

Figure 4: Flowchart of the Phased addition algorithm

Here *O* matrix is image matrix, *B*is reconstructed a-scan signal estimated for each pixel in the image domain, t_{peak} is the time of occurrence of peak in the transmitted signal, and $t_{max}$is the time of occurrence of maximum amplitude of each reconstructed a-scan. For each pixel in the image domain the amplitude value, at an "index" of the reconstructed a-scan, is read and assigned to the corresponding pixel in the imaging domain. The "index" used in the image reconstruction corresponds to the location of peak in the input signal.

3.3 Simulation studies: Comparison of single-quadrant double-ring STMR array and full-ring STMR array based on the reconstructed Image quality

Simulations have been carried out to demonstrate the applicability of a single sensor (the single-quadrant double-ring STMR array) for in-situ SHM of anisotropic structures and the reconstructed images are compared with the images reconstructed using simulation data of the full-ring STMR array configuration.

Two point defects, one at (0.3 m, 0.1 m) and the other at (-0.2 m, 0.3 m), on 3.15 mm quasi-isotropic composite are simulated using S_0 mode dispersion data for the two array configurations (single-quadrant double-ring STMR array and full-ring STMR array). S_0 mode dispersion properties are calculated by solving Rayleigh-Lamb equation. In the simulations, two-cycle tone burst signal of 200 kHz frequency is excited at the center of the array. The reflected signals from the defects are simulated as explained in Section 3.1 and are sampled at 2.5 Mega-sample/sec. For the two array configurations, simulated signals are used in phased addition algorithm to image the defects on the plate and the reconstructed images are shown in Fig. 5. Two images, shown in Fig. 5(a) and Fig. 5(b) are reconstructed using full-ring STMR array and single-quadrant double-ring STMR array respectively.

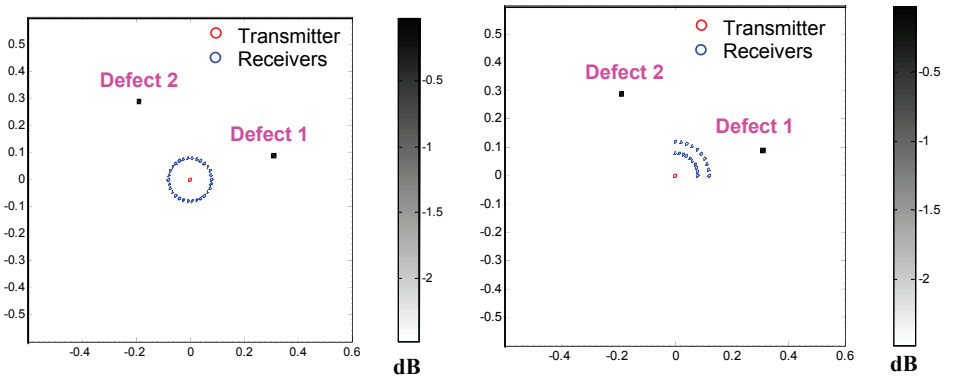

(a) Using full-ring STMR array (b) Using single-quadrant double-ring STMR array

Figure 5: Reconstructed defect images using S_0 mode dispersion data of the 3.15 mm graphite epoxy composite plate for (a) full-ring STMR array and (b) single-quadrant double-ring STMR array configurations. Defect1 = [0.3 m 0.1 m] Defect2= [-0.2 m, 0.3 m]

Similarly, two point defects, one at (0 m, 0.3 m) and the other at (-0.3 m, -0.3 m), on 3.15 mm quasi-isotropic composite are simulated using A_0 mode dispersion data for the two array configurations. Fig. 6(a) and Fig. 6(b) shows the images

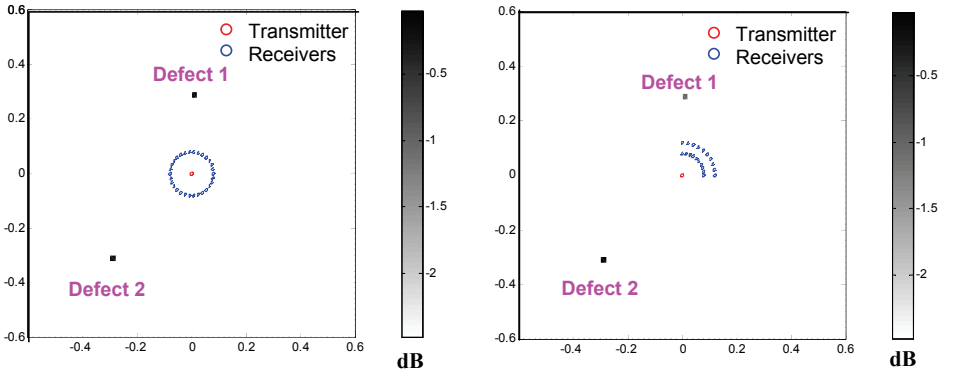

(a) using full-ring STMR array (b) using single-quadrant double-ring STMR array

Figure 6: Reconstructed defect images using A_0 mode dispersion data of the 3.15 mm graphite epoxy composite plate for (a) full-ring STMR array and (b) single-quadrant double-ring STMR array configurations. Defect1 = [0 m, 0.3 m] Defect2= [-0.30 m, -0.3 m]

reconstructed using phased addition algorithm for full-ring STMR array and single-quadrant double-ring STMR array configurations respectively. The difference in the decibel level of the two defects is -0.15 dB (for full-ring STMR array) and -0.98 dB (for single-quadrant double-ring STMR array).

The relative dB difference between a pair of point defects imaged with the single quadrant double ring STMR array was found to be consistently greater than that for the full ring STMR array. However, the dB difference for the single quadrant double ring was found to be of the same order of magnitude as that for the full ring, both being less than 0.1 dB. From the above two simulations, it was observed that, even with less number of sensors, single-quadrant double-ring STMR array (20 receivers) has performed equally well as the full-ring STMR array (30 receivers). Considering the fact that the single-quadrant double-ring STMR array has reduced electronics, reduced weight and smaller foot print, the single-quadrant double-ring STMR array appears to be an attractive option for in-situ SHM of anisotropic plate-like samples.

4 Experiments with single-quadrant double-ring STMR array

Two impact damages are created on 3.15 mm “quasi-isotropic” graphite-epoxy composite with different impact loads. The size of the delamination1 is 40 mm x 40 mm (created with impact load of 16 J) and delamination2 is 30 mm x 40 mm (created with impact load of 13 J) are obtained by carrying out ultrasonic C-scan

and are show in Fig. 7. The composite plate with the sensor array was shown in Fig. 2. Following the procedure outlined in Section 2, the experimental signals are sampled at 2.5 Mega-samples/sec using the DAQ card NI 5102. In the first step, elastic moduli were reconstructed from S_0 mode velocity data measured using the direct received signals at the two radii of the sensor array. In the second step, the defects were imaged using the phased addition algorithm on the signals received by the outer ring of sensors and the reconstructed elastic moduli obtained in the first step.

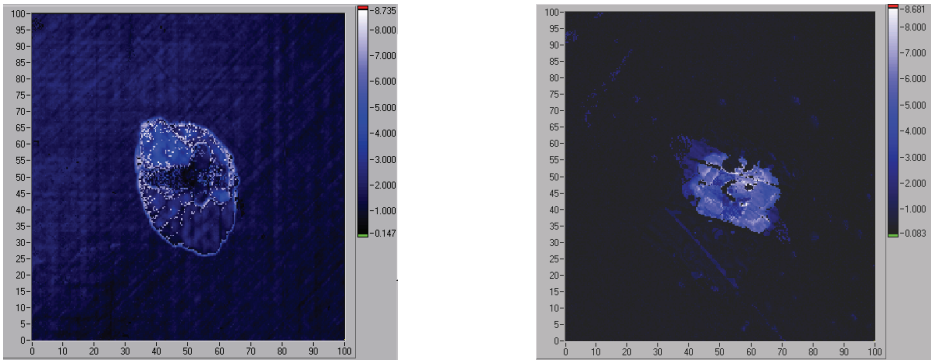

(a) Delamination1 (b) Delamination2

Figure 7: C-scan images of the 3.15 mm graphite epoxy composite plate (a) delamination1(40 mm x 40 mm), and (b) delamination2 (30 mm x 40 mm)

In order to image the edges and defects effectively from the measured signals, it is important to (i) remove the direct received signals from all the measured signals, and (ii) need to compensate for the shift in the effective source for the Lamb wave generation. The shift depends on the actual source distribution and the characteristics of the Lamb wave that is sought to be generated. The length of direct received signal can be estimated by calculating the velocity in that direction using the reconstructed elastic moduli. To remove the effect of direct received signal, the direct received signal is replaced by an array of zeros of that length. To account for the shift in the center of generation of Lamb waves, a time interval of "dt" was found to be sufficient to shift the effective source for the lamb waves from the location of the actual transduction. The time interval "dt" can be obtained using the wave speed and the distance between two sensors placed at a known distance apart along the wave propagation direction. For anisotropic materials, the numerical value of the "dt" varies with direction.

After removing the above two effects from the measured signals, modified signals

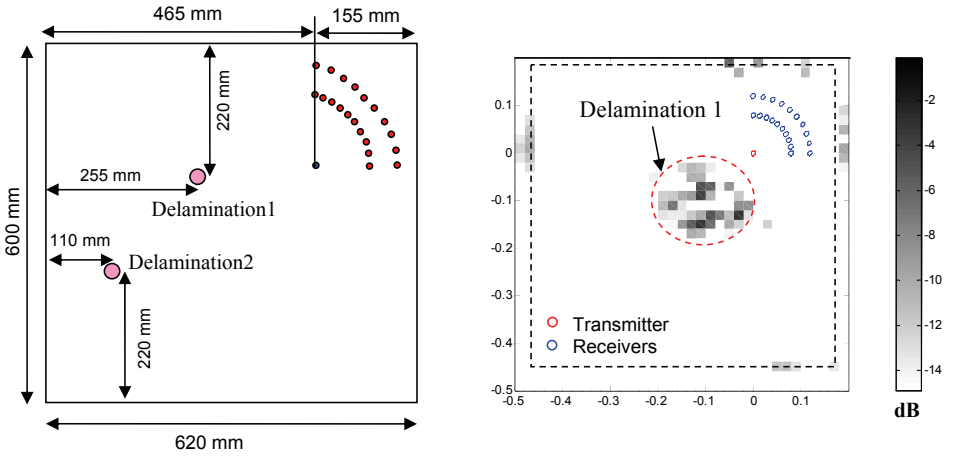

(a) (b)

Figure 8: Experimental reconstruction of defect images in the 3.15 mm graphite-epoxy composite plate using single-quadrant double-ring STMR array. (a) Schematic of the experimental set-up, and (b) Image reconstructed using experimental data

were given to the phased addition algorithm to image edges and defects present on the structure. Promising results were obtained using the single-quadrant double-ring STMR array. Fig. 8(a) shows the schematic of the experimental set-up and, Fig. 8(b) shows the reconstructed image using the experimental data. Dotted lines correspond to the plate edges. Four edges of the plate and one delamination (Delamination1) were imaged well. The farther defect (Delamination2) could not be reconstructed. It is likely that this defect is shadowed by the nearer defect (Delamination1).

5 Conclusions

A new sensor array (single-quadrant double-ring STMR array) has been developed for in-situ assessment of elastic moduli, material symmetry, orientation of principal planes and defect imaging. The direct received signals were used to determine elastic moduli whereas the reflected signals from the edges and defects along with the reconstructed elastic moduli were used in the phased addition algorithm to image defects on the plate-like structures. Reconstruction of elastic moduli of a graphite epoxy composite plate has been carried out by a Genetic Algorithm (GA) based inversion method using S_0 mode velocities measured in various directions of a quadrant.

Simulations of defects have been carried out to compare the performance of the single-quadrant double-ring STMR array against the performance of full-ring STMR array. From the reconstructed image contrast plots, it was observed that single-quadrant double-ring STMR array has performed equally well as the full-ring STMR array. The single-quadrant double-ring STMR array has several advantages over full-ring STMR array for in-situ SHM such as (i) compact foot-print, (ii) reduced weight of sensor array, (iii) reduced electronics, (iv) greater coverage, as the geometry allows it to be placed in the vicinity of structural features – e.g., plate edges, and (v) an ability to determine elastic moduli in-situ.

From the experimental signals, it was observed that lamb wave generation appeared to be generated from an effective source that was shifted from the actual location of the transmitting actuator element. This positional shift could be ascertained and was needed for all the calculations to obtain the correct elastic moduli and proper image reconstruction. Through experiments, it was demonstrated that single-quadrant double-ring STMR array is capable of in-situ SHM of anisotropic plate-like structures.

Acknowledgement: The authors thank the Advanced Composite Division of the National Aeronautical Laboratory, Bangalore for providing the composite samples, and Aeronautical Development Agency, Bengaluru for funding this research work.

References

Cowin, S. C.; Mehrabadi, M. M. (1987): On the identification of material symmetry for anisotropic elastic materials. *The Quarterly Journal of Mechanics and Applied Mathematics*, vol. 40, no. 4, pp. 451-476.

Giurgiutiu, V. (2005): Tuned Lamb wave excitation and detection with piezoelectric wafer active sensors for structural health monitoring. *Journal of Intelligent Material Systems and Structures*, vol. 16, no. 4, pp. 291-305.

Giurgiutiu, V.; Zagrai, A. N.; Bao, J. J. (2002): Piezoelectric wafer embedded active sensors for aging aircraft structural health monitoring. *Structural Health Monitoring* , vol. 1, no. 1, pp. 41-61.

Goldberg, D. E. (1989): *Genetic Algorithms in Search, Optimization, and Machine Learning* (Reading, MA: Addison-Wesley)

Ihn, J. B.; Chang, F. K. (2004): Detection and monitoring of hidden fatigue crack growth using a built-in piezoelectric sensor/actuator network: I. Diagnostics. *Smart Materials and Structures*, vol. 13, no. 3, pp. 609-20.

Jagannathan, R.; Balasubramaniam, K.; Krishnamurthy, C. V. (2006): A phase reconstruction algorithm for Lamb wave based structural health monitoring

of anisotropic multilayered composite plates. *Journal of the Acoustical Society of America*, vol. 119, no. 2, pp. 872-78.

Kawiecki, G. (1998): Feasibility of applying distributed piezotransducers to structural damage detection. *Journal of Intelligent Material Systems and Structures*, vol. 9, no. 3, pp. 189–97.

Kessler, S. S.; Spearing, S. M.; Soutis, C. (2002): Damage detection in composite materials using Lamb wave methods. *Smart Materials and Structures*, vol. 11, pp. 269-78.

Kuang, K. S. C.; Cantwell, W. J. (2003): Use of conventional optical fibers and fiber Bragg gratings for damage detection in advanced composite structures: A review. *Applied Mechanics Review*, vol. 56, no. 5, pp. 493-513.

Lin, M.; Chang, F. K. (2002): The manufacture of composite structures with a built-in network of piezoceramics. *Composites Science and Technology*, vol. 62, no. 7-8, pp. 919-39.

Lynch, J. P.; Loh, K. J. (2006): A summary review of wireless sensors and sensor networks for structural health monitoring. *The Shock and Vibration Digest*, vol. 38, no. 2, pp. 91-128.

Montalvão, D.; Maia, N. M. M.; Ribeiro, A. M. R. (2006): A review of vibration-based structural health monitoring with special emphasis on composite materials. *The Shock and Vibration Digest*, vol. 38, no. 4, pp. 295–324.

Muralidharan, A.; Balasubramaniam, K.; Krishnamurthy, C.V. (2008): A migration based reconstruction algorithm for the imaging of defects in a plate using a compact array. *Smart Structures and Systems*, vol. 4, no. 4, pp. 449-64.

Nayfeh, A. H. (1995): *Wave Propagation in Layered Anisotropic Media with Application to Composites* (Amsterdam: Elsevier Publication)

Pawar, P. M.; Ganguli, R. (1997): Helicopter rotor health monitoring – a review. *Proceedings of the Institution of Mechanical Engineers*, *Part G: Journal of Aerospace Engineering*, vol. 221, no. 5, pp. 631-47.

Qing, X.; Kumar, A.; Zhang, C.; Gonzalez, I. F.; Guo, G.; Chang, F. K. (2005): A hybrid Piezoelectric/Fiber optic diagnostic system for structural health monitoring. *Smart Materials and Structures*, vol. 14, pp. S98-S103.

Soma Sekhar, B. V.; Balasubramaniam, K.; Krishnamurthy, C. V. (2006): Structural Health Monitoring of fiber-reinforced composite plates for low-velocity impact damage using ultrasonic Lamb wave tomography. *Structural Health Monitoring*, vol. 5, no. 3, pp. 243-53.

Vishnuvardhan, J.; Krishnamurthy, C. V.; Balasubramaniam, K. (2007a): Genetic algorithm based reconstruction of the elastic moduli of orthotropic plates

using an ultrasonic guided wave single-transmitter-multiple-receiver SHM array. *Smart Materials and Structures*, vol. 16, pp. 1639-50.

Vishnuvardhan, J.; Krishnamurthy, C. V.; Balasubramaniam, K. (2007b): Genetic algorithm reconstruction of orthotropic composite plate elastic constants from a single non-symmetric plane ultrasonic velocity data. *Composites Part B: Engineering*, vol. 38, no. 2, pp. 216-27.

Vishnuvardhan, J.; Krishnamurthy, C. V.; Balasubramaniam, K. (2009a): Blind inversion method using Lamb waves for the complete elastic property characterization of anisotropic plates. *Journal of Acoustic society of America*, vol. 125, no. 2, pp. 761-71.

Vishnuvardhan, J.; Muralidharan, A.; Krishnamurthy, C. V.; Balasubramaniam, K. (2009b): Material characterization and SHM of orthotropic plates through an ultrasonic guided wave STMR array. *NDT&E International*, vol. 42, no. 3, pp. 193-98.

Wilcox, P. D. (2003a): Guided wave beam steering from omnidirectional transducer arrays. *Review of Progress in Quantitative Nondestructive Evaluation*, vol. 22, pp. 761-68.

Wilcox, P. D. (2003b): Omnidirectional guided wave transducer arrays for the rapid inspection of large areas of plate structures. *IEEE Transactions on Ultrasonics, Ferroelectrics, and Frequency Control*, vol. 50, no. 6, pp. 699-709.

Wilcox, P. D.; Lowe, M.; Cawley, P. (1999): Lamb and SH wave transducer arrays for the inspection of large areas of thick plates. *Review of Progress in Quantitative Nondestructive Evaluation*, vol. 19, pp. 1049–56.

Zhou, Y; Qiao, Y. Krishnaswamy, S. (2006): Adaptive demodulation of dynamic signals from fiber Bragg gratings using two-wave mixing technology. *Applied Optics*, vol. 45, no. 21, pp. 5132-42.